RF/Optical Hybrid Antenna

Troy M. Torrez*

ABSTRACT. — This article details analyses performed on several variations of a proposed radio frequency (RF)/optical hybrid antenna. The goal was to determine the structural impact of adding an assembly of optical mirrors to the antenna; stresses in the structural members and reflector surface deformation were used to assess this impact. The results showed that the structure could handle the added assembly, and the surface RMS increased, as expected, with larger increases seen as the antenna translates in elevation from the rigging angle of 45 deg (a predetermined location chosen to optimize panel settings during installation). In addition, actuators are located behind each optical mirror to reoptimize the mirror positions after they deflect due to the antenna being tipped in elevation. The necessary actuator motion was calculated for each mirror for a range of elevation angles, and it was found that the required motions are achievable by commonly used actuators. Resonant frequency analysis was also performed on the quadripod and tripod (for DSS-13 at Goldstone) to determine the effect that adding optical components on the apex has on the structure and its first mode; it was found that the impact is minimal to both the stresses seen in the structure and its first mode.

I. Introduction

Deep-space optical communication is widely recognized as an important technology development area for future NASA space exploration missions due to the high data rates it promises. Optical communication links are most suitable for high-rate, high-volume science downloads that can be scheduled with some flexibility. Standard spacecraft tracking, telemetry, and command functions, including emergency and safe-mode communications, are better suited to radio frequency (RF) links that are more robust under a wide range of weather conditions. These different characteristics of RF and optical communications pose challenges and lead to operations concepts that utilize simultaneous optical and RF communications.

One of the possible ground station concepts under consideration is a unique RF/optical ground station for reception of high-bandwidth optical deep-space communications and simultaneous support of conventional RF uplink and downlink [1,2]. This approach inte-

* Communications Ground Systems Section.

The research described in this publication was carried out by the Jet Propulsion Laboratory, California Institute of Technology, under a contract with the National Aeronautics and Space Administration.

grates a segmented optical primary surface onto the main reflector of an existing antenna designed for RF operations and an RF/optical beam splitter into the RF antenna's subreflector (Figure 1). The shape of the optical primary surface is maintained with an actuation system that aligns each segment of the optical primary. Finally, the shape of the antenna's main RF reflector and subreflector are adjusted in order to optimize the antenna's RF performance in this new hybrid configuration.

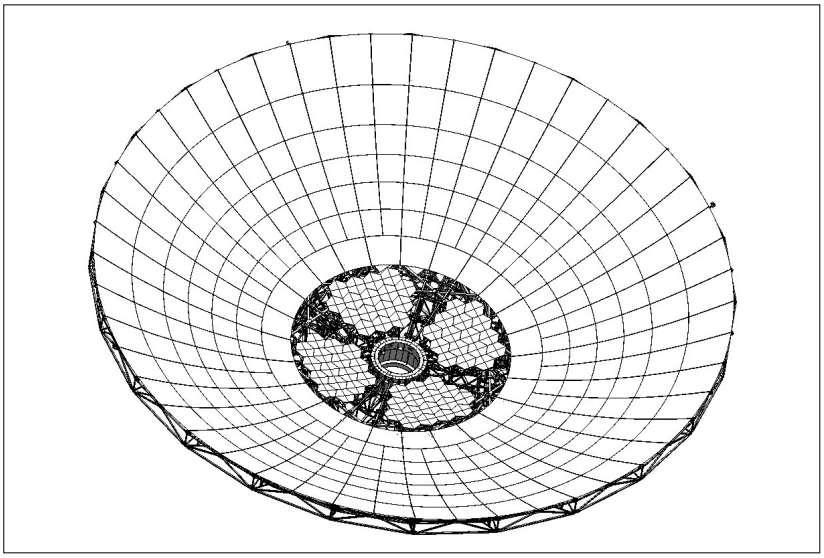

Figure 1. RF/optical hybrid antenna reflector.

Successful implementation of such a ground station requires unique optical design and a control and actuator system for panel alignment, as well as mechanical/structural design and analysis. In this article, we describe some of the mechanical analyses of the RF/optical ground station that have been completed to date.

Removal of the inner rows of RF panels and adding the optical assembly results in a major modification of the loading on the antenna's backup structure. This new loading impacts the safety margin of the structure, affects the RF performance of the structure, and determines the design of the optical actuator system. In order to quantify how the modifications affect the antenna's performance and the structure's ability to handle the additional weight, several analyses were performed. These analyses include: (1) structural load analysis, (2) computation of RF surface distortion versus elevation angle, and (3) computation of the required actuator motion to reposition optical panels versus elevation angle. The following sections describe in detail the results of these analyses.

II. General Layout and Fit

The existing design for the primary reflector of the 34-m beam-waveguide (BWG) antenna comprises nine rows of panels; each row of panels is laid out in the circumferential direction. In order to accommodate the optical assembly, the inner two rows of panels are removed. The optical assembly on the primary is made up of 64 mirrors and a support-

ing structure. Figure 2 shows a side view of the antenna, depicting the primary RF surface, spherical optical surface in the center, RF/optical splitting surface on the RF secondary, and the spherical aberration corrector behind the secondary.

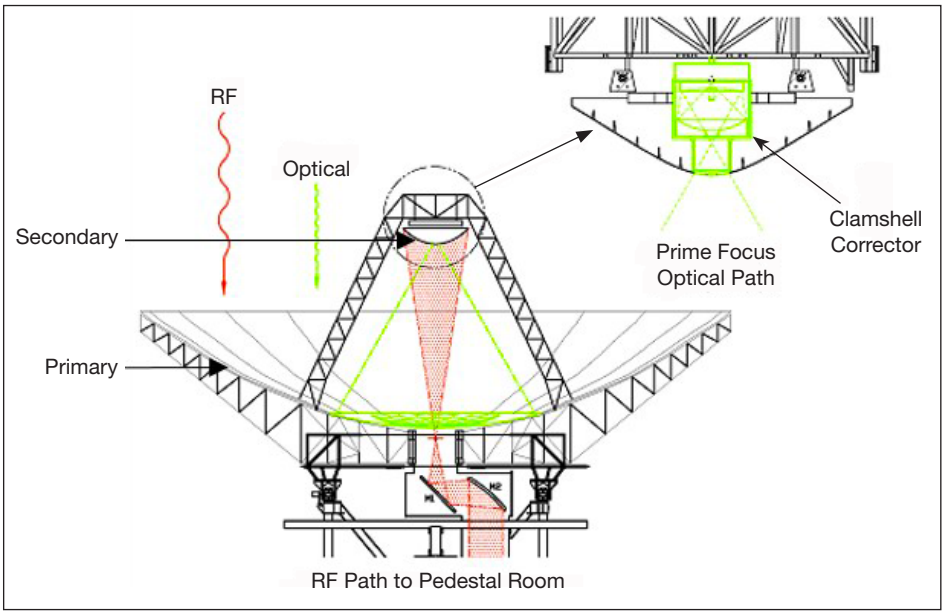

Figure 2. Side view of the RF/optical concept, including ray paths.

The 64 optical mirrors are divided into four pods of 16 mirrors. Each pod is supported by a frame assembly of structural beams, which tie the optical assembly into the reflector backup structure. Each mirror is supported by three actuators and a backup plate, which then tie into the supporting structure of the optical assembly.

III. Analyses

A. Structural Analysis

In order to check the structural impact that adding the optical assembly has on the antenna, a stress analysis was performed on the structure; the finite-element model used in this analysis is shown in Figure 3. A factor of safety of two was required for all members in order for the structure to pass. The antenna was analyzed in different orientations because the loading on the members is altered depending on how the antenna is oriented; the antenna was analyzed for elevation angles from 10 deg to 90 deg. It was found that all of the members had factors of safety greater than two for all elevation angles.

B. RF Surface Distortions

The distortion and movement of the RF panels was quantified by performing a root-mean-square (RMS) calculation of the nodes representing the corners of the panels. The required data for this calculation is extracted from the results of the analyses described in the prior section. The coordinates and displacements of the nodes were used as inputs in a MATLAB script taken from [3].

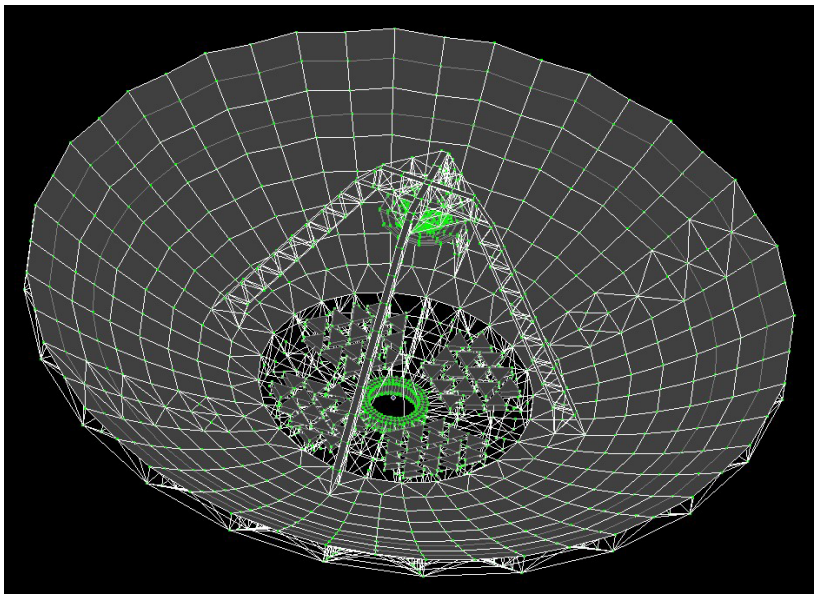

Figure 3. RF/optical hybrid antenna finite-element model.

In order to compare how modifying the structure impacts the surface RMS, the calculations were performed for three cases: existing BWG, hybrid BWG with optical assembly, and hybrid high-efficiency (HEF) with optical assembly. The HEF antennas are quite different from the BWG antennas since they do not require a central beam waveguide hole, and operate with a conventional feed cone arrangement on the primary surface. The results are shown in Figure 4.

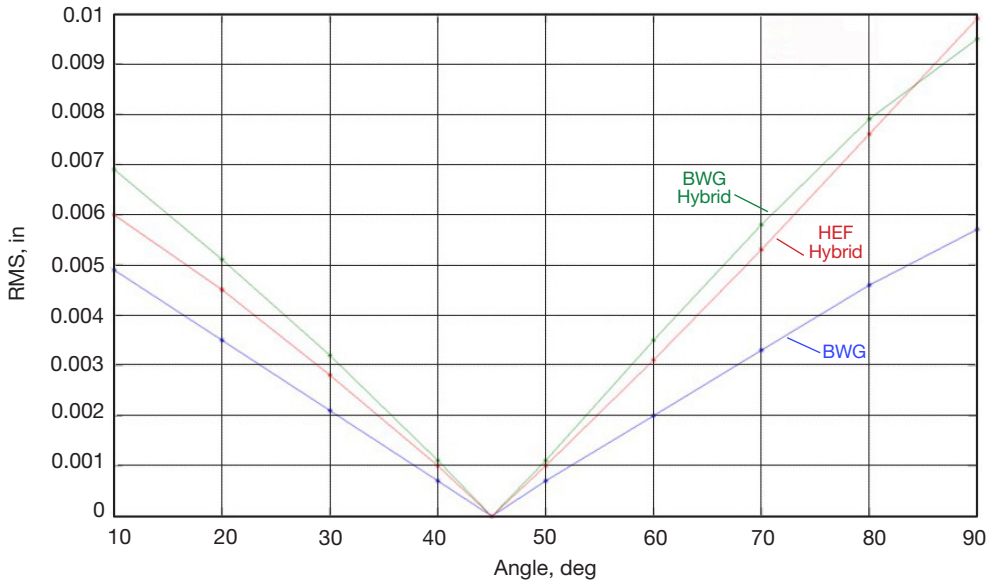

Figure 4. Surface RMS for range of elevation angles.

The surface RMS of the hybrid BWG and the hybrid HEF is greater than that of the BWG, as expected. Because the inner rows of panels are removed in the hybrid design, and these panels undergo the least distortion, the surface RMS for the hybrid antennas was expected to be greater than in the BWG. Also, adding the optical assembly contributes to the increase in the surface RMS because of the weight that is being added to the structure. This increase in surface RMS for the hybrid designs equates to a maximum loss of approximately 0.4 dB at 90 deg elevation at 32 GHz. This loss could be either accommodated in the link budget or recovered by slightly increasing the size of the primary reflector in future implementation.

C. Optical Panel/Actuator Motions

Due to deflection in the frame assembly of the optical assembly, the optical mirrors no longer lie on the required sphere. To reposition the mirrors on the sphere, the actuators that lie behind the mirrors must piston the appropriate amount; each mirror is moved by three actuators. In order for the mirrors to be properly repositioned, the actuators must have enough linear throw to create the required mirror motion.

From the structural analysis, the required data were collected and processed in MATLAB to determine the required actuator motions. Three nodes on the top face of each mirror were tracked; three nodes were required because a plane needs to be created in the subsequent calculations. The coordinates and displacements of the nodes from the finite-element analyses for the range of elevation angles were collected.

To determine the required actuator motions, a MATLAB script was written. The script performed vector analysis to determine the required angle and normal motion to return the mirror to the sphere. The following is the process that the MATLAB script followed. From the RF surface RMS calculations, the required motion of the subreflector was outputted by the MATLAB script. Because the optics in the secondary lie behind the subreflector, they undergo the same motion as the subreflector. The center of the optical sphere was taken to have moved by the same distances in all directions. The new position of each mirror was calculated based on the displacements of the three nodes that lie on their top faces. For each mirror, the vector normal to the top surface and passing through the center point was calculated. Next, the vector from this center point to the center of the optical sphere was calculated. The angle between these two vectors was calculated, which represents the amount of rotation the mirror must undergo. Also, using the vector from the center of the mirror to the optical sphere center, the distance from the mirror center to the surface of the sphere was calculated; this represents the required normal motion of the mirror. The required rotation and normal motion was calculated for all 64 mirrors for each elevation angle. For each elevation angle, the maximum rotation and maximum normal motion was calculated. While not always true, it was assumed that the maximum rotation and maximum normal motion coincided on the same mirror. If the actuators have the required throw to create this mirror motion, the frame assembly of the optical assembly provides an acceptable stiffness to resist motion due to gravitational loads in varying orientations of the antenna.

The results of this analysis are shown in Figure 5. The required actuator motion for the HEF design is approximately 0.36 in and for the BWG hybrid design is approximately 0.68 in. These motions are easily achieved by a number of commercial actuators.

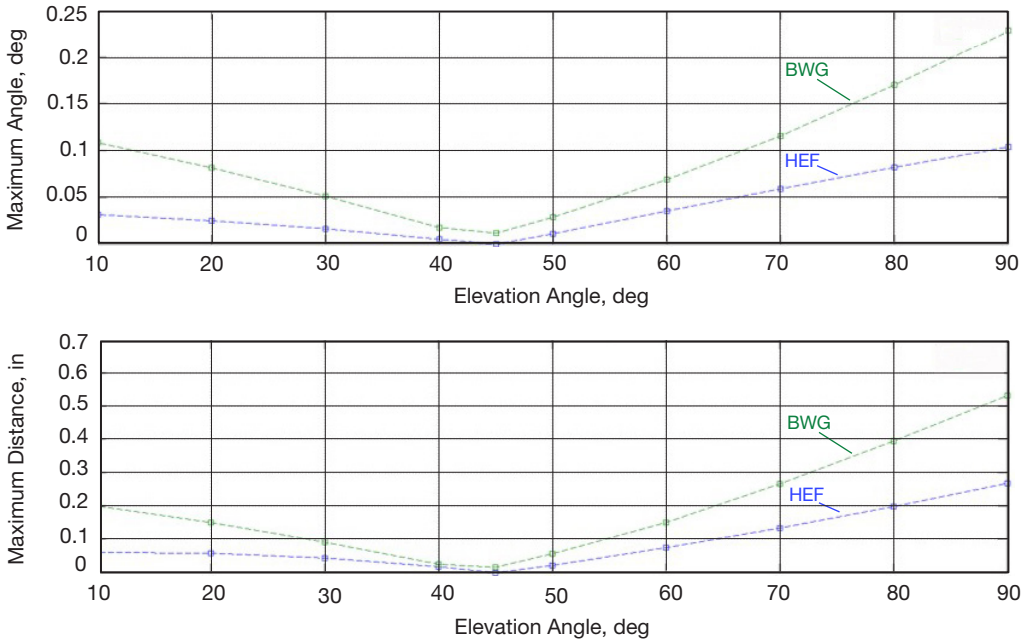

Figure 5. Required mirror motion for range of elevation angles.

D. Resonant Frequencies

In a separate analysis, the resonant frequencies of the tripod/quadripod were determined using finite-element analysis. The first goal was to determine what effect, if any, modifying the secondary to include optics has on the resonant frequencies on the tripod/quadripod. The second goal was to see if the mode shapes helped to explain vibrations seen in video taken from the secondary on DSS-13 at Goldstone; DSS-13 has a tripod while the current BWG design has a quadripod. Table 1 and Table 2 list the modes for the tripod and quadripod.

Figure 6 shows the first mode of the tripod; this mode is a twisting mode about an axis passing through the center of the structure. As seen in Figure 2, the clamshell corrector is positioned in the center of the secondary. Therefore, given the centered optical design, the first mode will not, to the first order, affect the clamshell corrector's ability to receive the signal. Also, this pure rotation mode provides an explanation for the vibrations seen in the video taken from the secondary on DSS-13.

Figure 7 shows the first mode of the quadripod; this mode is a twisting mode similar in shape to that of the tripod. The model was analyzed in two configurations: one with and one without the added weight for the optical hardware in the secondary. It was found that the added weight had no significant effect on the structural integrity of the quadripod or the frequency at which the first mode occurs. For the case of a centered optical system,

Table 1. Modes of tripod.

Mode Number	Frequency, Hz	Shape
1	2.38	Pure rotation
2	5.23	Bending of two legs
3	5.24	Bending of three legs
4	8.41	Pure rotation

Table 2. Modes of quadripod.

Mode Number	Frequency, Hz	Shape
1	2.96	Pure rotation
2	6.12	Bending of two opposite legs
3	6.26	Bending of two opposite legs
4	7.48	Bending of four legs in symmetric manner
5	9.46	Bending of two opposite legs
6	9.68	Bending of two opposite legs

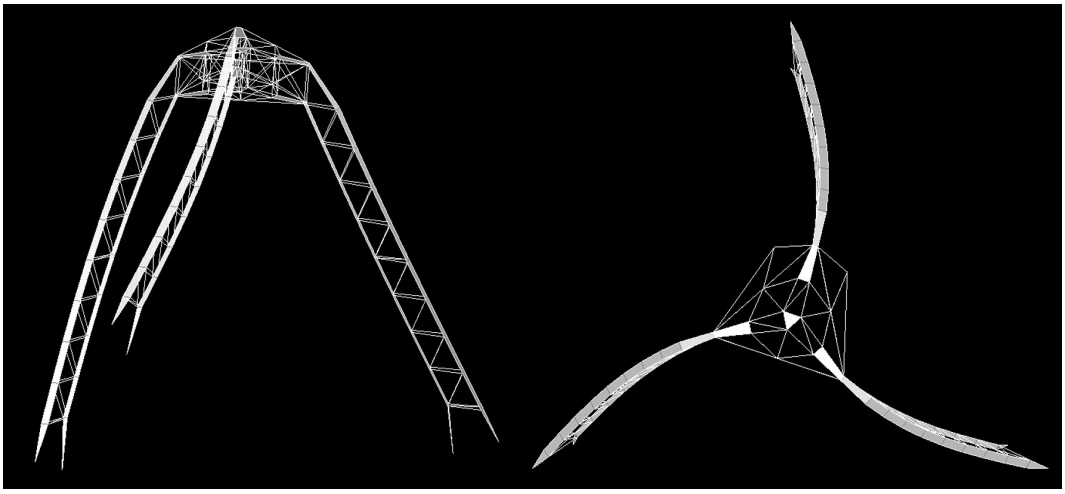

Figure 6. Tripod first mode.

the first mode of concern is mode #2 in either case with a resonant frequency of 5.23 or 6.12 Hz, depending on the strut configuration. It should be noted that no significant oscillation at this second mode (5.23 Hz) has been observed during experiments at DSS-13 to date.

Work is currently underway to remove the effects of these resonances through the addition of a fast-steering mirror in the optical train. Such a system can easily accommodate all of the resonant frequencies in Table 2.

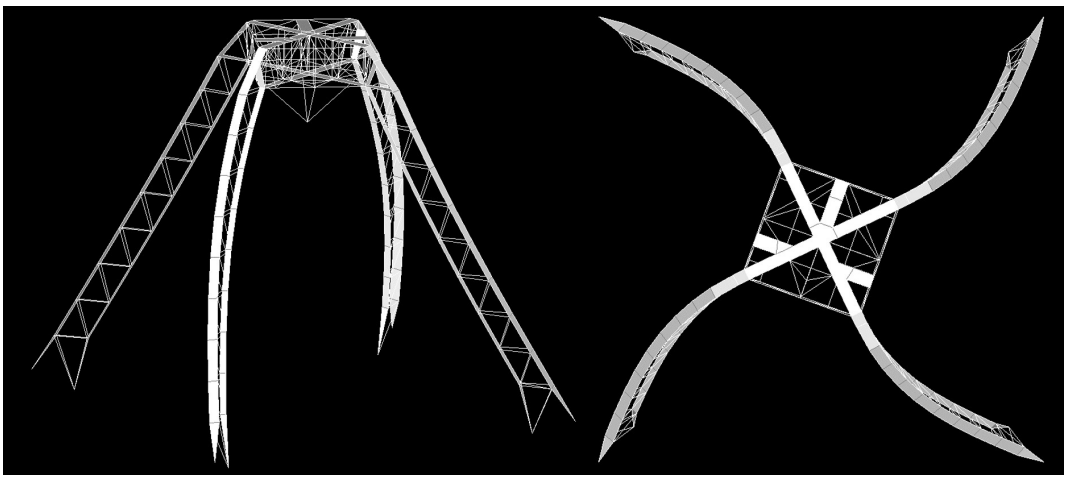

Figure 7. Quadripod first mode.

IV. Conclusions

In this article, a BWG hybrid antenna and a HEF hybrid antenna were analyzed and compared to existing designs where appropriate. Stresses in the structural members and reflector surface deformation were used to assess the impact of adding an assembly of optical mirrors to the antenna. The results showed that the structure could handle the added assembly, and the surface RMS increased, as expected, with larger increases seen as you move away from the rigging angle of 45 deg. As the antenna is being tipped through elevation, the optical mirrors deflect, and actuators located behind each mirror are used to reposition the mirrors. The necessary actuator motion was calculated for each mirror for a range of elevation angles, and it was found that the required motions are achievable by commonly used actuators. Resonant frequency analysis was also performed on the quadripod and tripod (for DSS-13) to determine the effect that adding optical components on the apex has on the structure and the first mode of the quadripod/tripod. It was found that these additional components have a minimal impact on the structure and its first mode.

V. References

[1] D. Hoppe, J. Charles, S. Piazzolla, F. Amoozegar, M. Britcliffe, and H. Hemmati, "Integrated RF/Optical Ground Station Technology Challenges," *The Interplanetary Network Progress Report*, vol. 42-181, Jet Propulsion Laboratory, Pasadena, California, pp. 1–38, May 15, 2010.
http://ipnpr.jpl.nasa.gov/progress_report/42-181/181B.pdf

[2] J. R. Charles, D. J. Hoppe, and A. Sehic, "Hybrid RF/Optical Communication Terminal with Spherical Primary Optics for Optical Reception," *Proceedings 2011 International Conference on Space Optical Systems and Applications (ICSOS)*, pp. 171–179, Santa Monica, California, May 11, 2011.

[3] R. Levy, *Structural Engineering of Microwave Antennas: For Electrical, Mechanical, and Civil Engineering*, IEEE Press, February 1996.